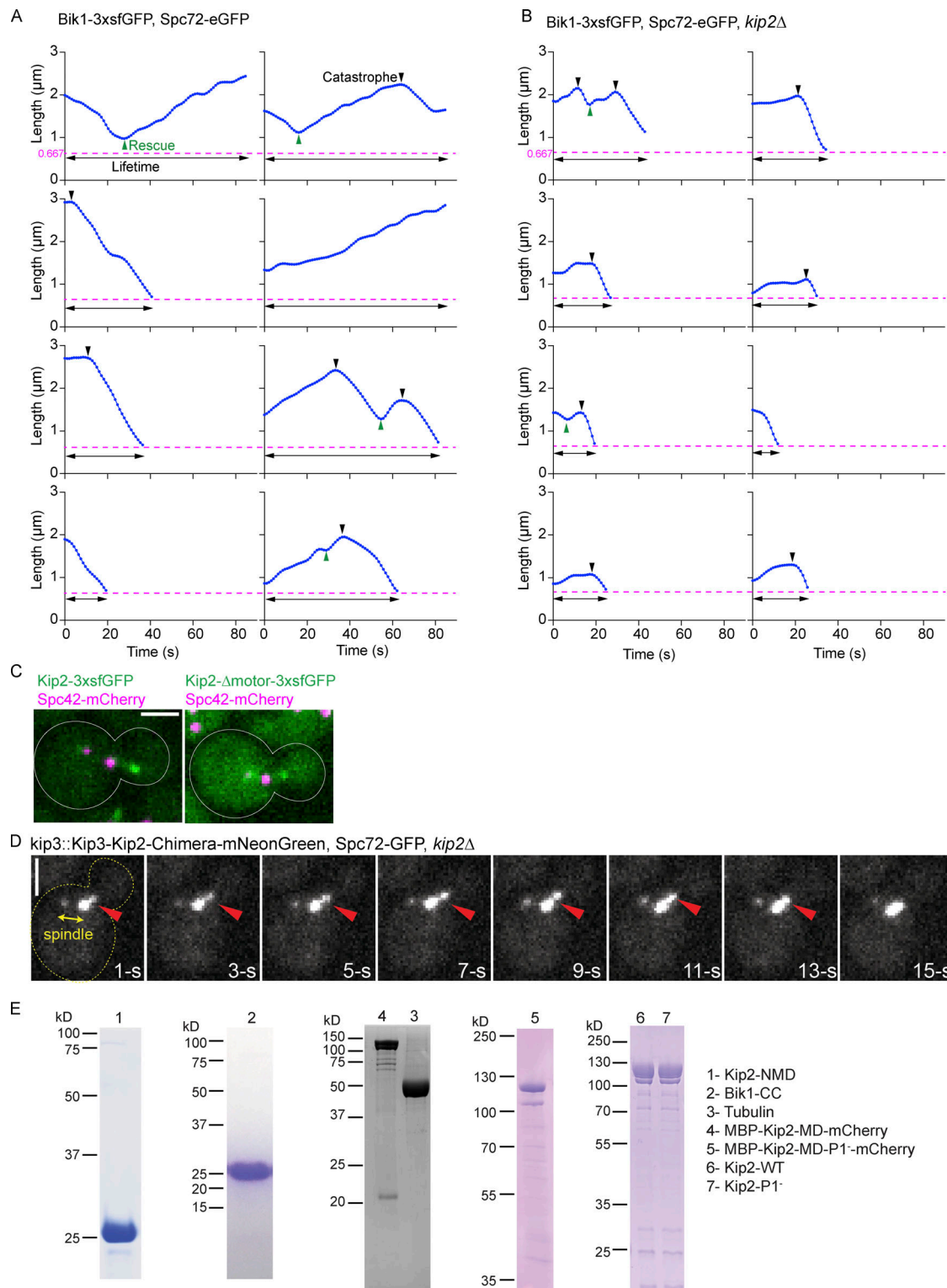
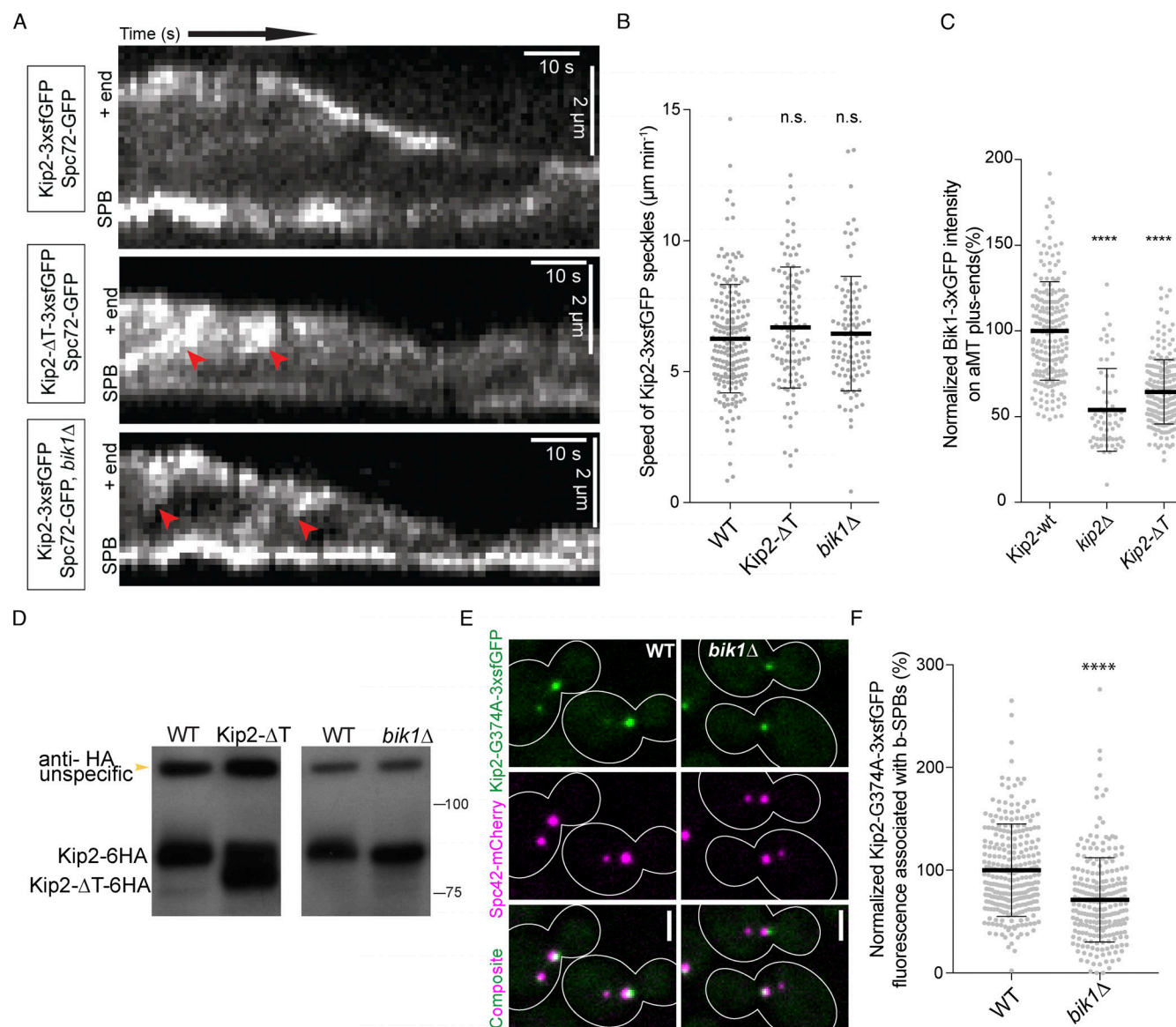


## Supplemental material



**Figure S1. Representative 3D aMT length tracking results, distribution of Kip2 mutants along microtubules, and SDS-PAGE of proteins used in vitro assays.** (A and B) Representative 3D aMT length was extracted from control (A) and *kip2Δ* (B) cells using Bik1-3xsfGFP and Spc72-eGFP as microtubule plus- and minus-end markers, respectively. The detection limit (666.7 nm due to the microscope resolution) is marked as a magenta dashed line. Rescue (green) and catastrophe (black) events are marked with triangles. The lifetime of each aMT is indicated with a black line with two arrowheads. (C) Representative images of full-length Kip2-3xsfGFP and Kip2-Δmotor-3xsfGFP accumulation on microtubule tips. (D) The chimera protein is composed of Kip3-MD and Kip2-NMD, then C-terminally fused with mNeonGreen, expressed from *KIP3* locus. The red arrowhead marks the plus-end of the aMT. SPBs are visualized with Spc72-GFP. Corresponds to Video 1. The time-lapse movie has 1.07 s intervals; only representative time points are shown here. Scale bar, 2 μm. (E) Coomassie-Blue-stained SDS-PAGE analysis of indicated proteins. Details of the constructs are summarized in Table S3. The Kip2-NMD image was cropped from the gel shown in Fig. 2 C. Source data are available for this figure: SourceData F51.



**Figure S2. The Kip2-Bik1 interaction is not required for efficient targeting of Kip2, but of Bik1, to microtubule plus-ends.** (A) Representative kymographs drawn from time-lapse series of preanaphase cells of the indicated genotype. SPBs were visualized with Spc72-GFP. Red arrowheads denote the speckles that appeared along the shaft of microtubules. (B) Quantification of Kip2 speckle moving speed using the kymographs shown in A. More than 90 speckles analyzed per condition. (C) Measurements of Bik1-3xGFP fluorescence intensity (%) on cytoplasmic microtubule plus-ends in cells of the indicated genotype. More than 90 cells analyzed per condition. (D) Western blot analysis of endogenously expressed Kip2-6HA and Kip2-ΔT-6HA. Lysates were prepared from cycling cells of the indicated genotype. (E) Representative images of preanaphase cells expressing the SPB marker Spc42-mCherry (magenta) and the ATPase deficient variant Kip2-G374A-3xsfGFP (green) in the presence and absence of Bik1. (F) Measurements of Kip2-G374A-3xsfGFP fluorescence intensity (%) associated with b-SPBs in cells shown in E. More than 90 speckles cells per condition. Statistical significance was calculated using two-tailed Student's *t* test. \*\*\*\*  $P < 0.0001$ ; n.s., not significant. Source data for B, C, and F are available in Data S1. Source data are available for this figure: SourceData FS2.

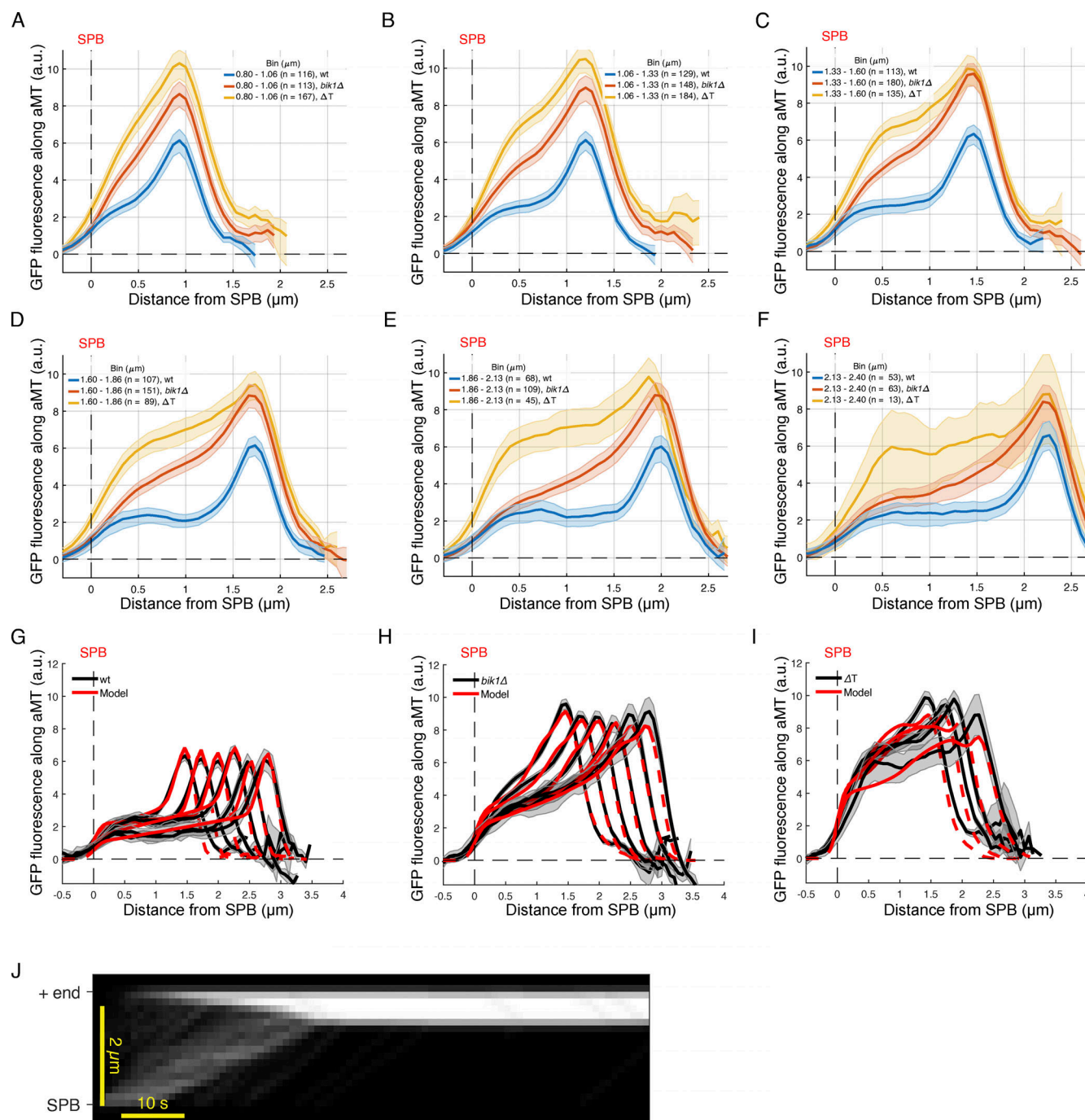


**Figure S3. Experimental and estimate results of Kip2 distribution along microtubules.** (A–F) Quantifications of fluorescence intensities (a.u.) from endogenous Kip2- $\Delta T$ -3xsfGFP and Kip2-3xsfGFP in the presence or absence of Bik1 along preanaphase cytoplasmic microtubules binned by microtubule length: (A) 0.80–1.06  $\mu\text{m}$ , (B) 1.06–1.33  $\mu\text{m}$ , (C) 1.33–1.60  $\mu\text{m}$ , (D) 1.60–1.86  $\mu\text{m}$ , (E) 1.86–2.13  $\mu\text{m}$ , (F) 2.13–2.40  $\mu\text{m}$ . (G–I) Experimental Kip2- $\Delta T$ -3xsfGFP (H), Kip2-3xsfGFP in the presence (G) or absence (I) of Bik1 fluorescence (a.u.) mean profile (black) and standard error (gray) with respective mean in silico estimation fits (red) for microtubules binned by length. Red dashed lines past plus-end and SPB indicates estimation extrapolations without support by data. (J) In silico kymograph with on rate constant of  $6.1\text{E-}4$  ( $\text{nM Kip2}^{-1} \text{s}^{-1}$ ), in rate constant of  $3.1\text{E-}1$  ( $\text{nM Kip2}^{-1} \text{s}^{-1}$ ), off rate constant of  $2.3\text{E-}2 \text{s}^{-1}$ , and total Kip2 concentration of 35 nM.



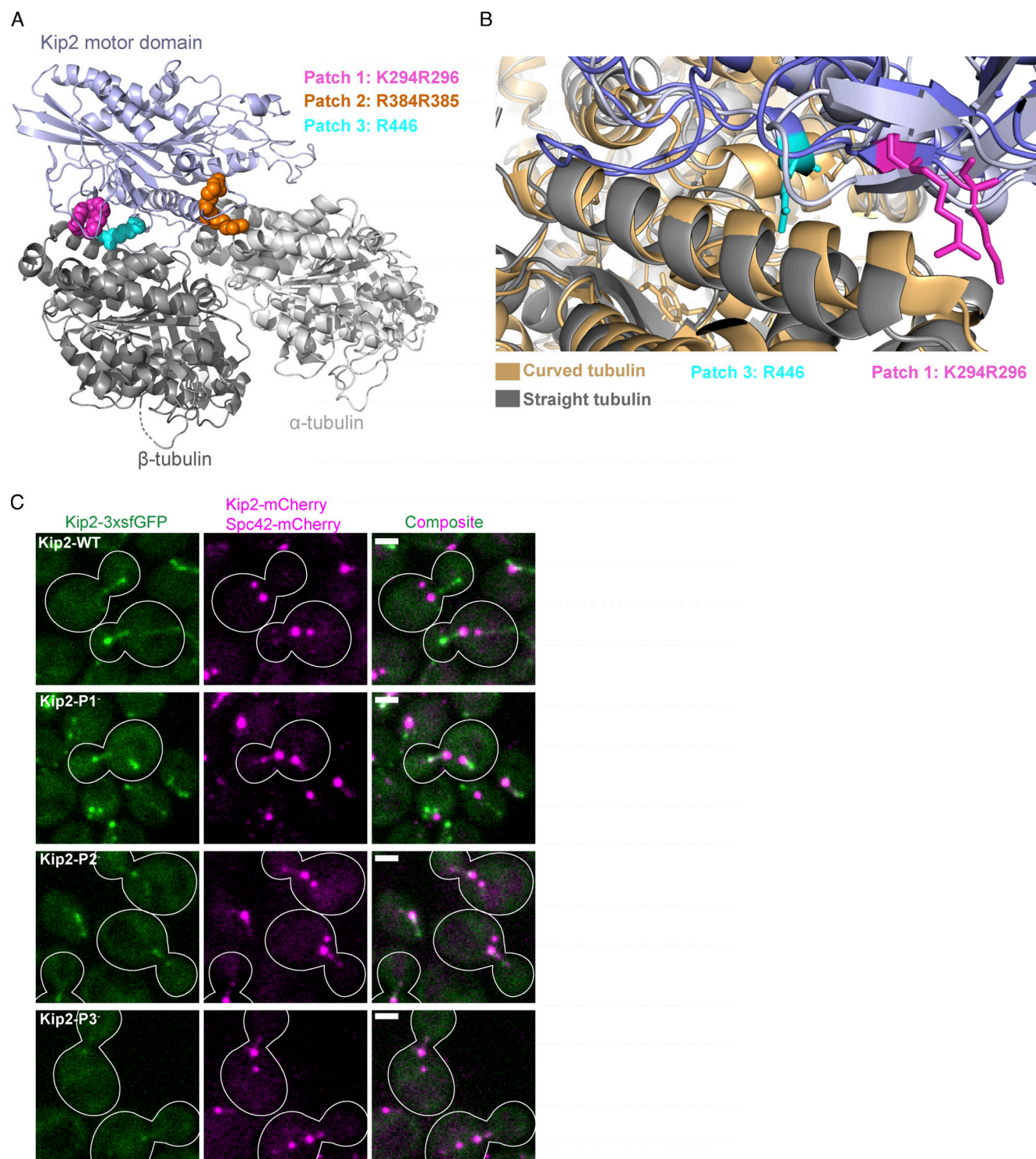


**Figure S4. Details of tubulin-bound Kip2-MD homology model and effects of indicated mutants in heterozygous yeast cells.** (A) Kip2-MD homology model (blue) in complex with a  $\alpha\beta$ -tubulin (gray) heterodimer. The three positively charged Kip2-MD surface patches that are crucial for tubulin or microtubule binding are highlighted in different colors (see corresponding legend). (B) Predicted binding of Kip2-MD (blue) to the curved (brown) and straight (gray) conformational states of tubulin. Residues K294 and R296 (P1, purple) and R446 (P3, sky blue) are highlighted to illustrate that P1 may selectively bind to the curved conformation of tubulin. (C) Localization of the wild-type and the tubulin-binding patch mutants of Kip2 in heterozygous diploid cells. Representative images of preanaphase heterozygous diploid cells expressing wild-type and tubulin-binding patch mutants of Kip2 fused to 3xsfGFP (green), together with wild-type Kip2 fused to mCherry. SPBs are visualized with Spc42-mCherry (magenta). Scale bars, 2  $\mu$ m.

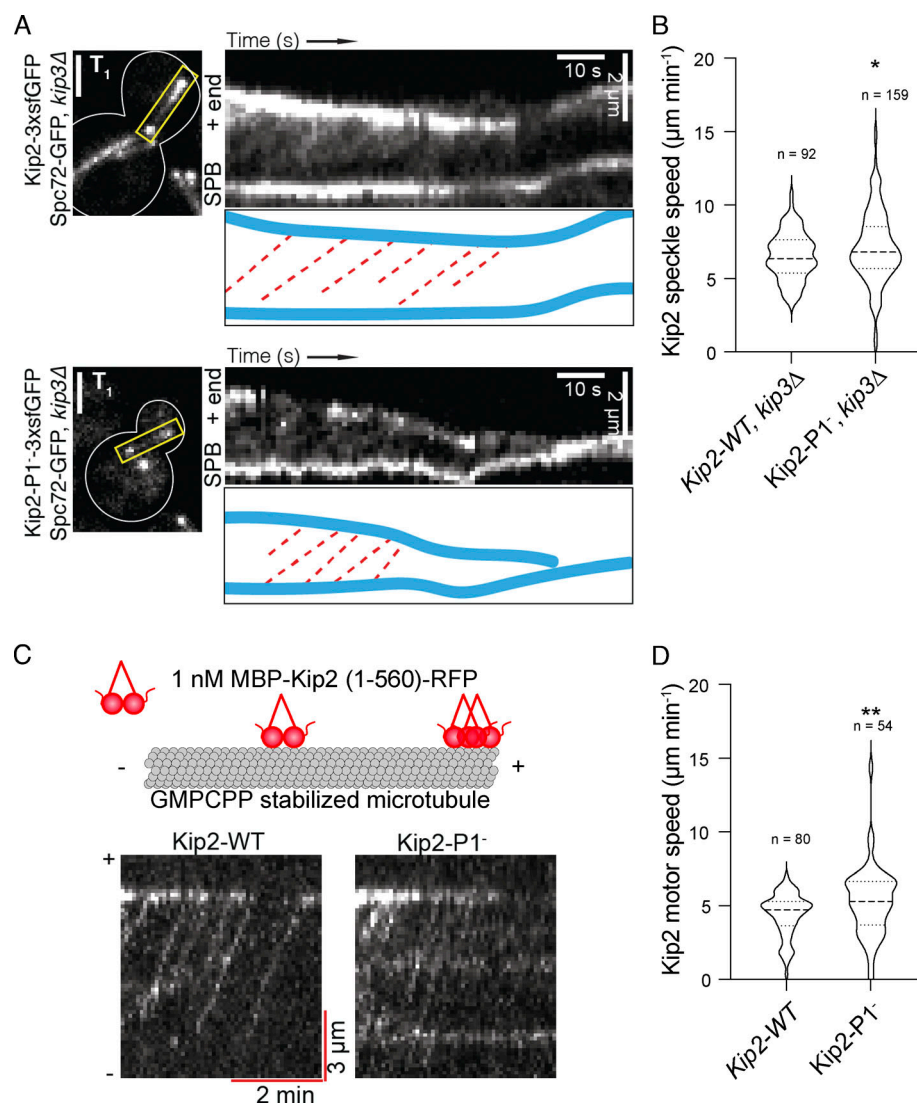


Figure S5. **Kip2 residues K294 and R296 are dispensable for Kip2 motility in vivo and in vitro.** (A) Representative preanaphase cells ( $T_1$ : the first frame), kymographs drawn from time-lapse series, and highlighted trajectories (red dashed lines) of Kip2-3xsfGFP (top) and Kip2-P1<sup>-</sup>-3xsfGFP (bottom) speckles moving along a metaphase aMT. Spc72-GFP was used to visualize SPBs. *KIP3* was deleted to increase the aMT length. Scale bars, 2  $\mu$ m. (B) Quantification of Kip2 speckle moving speed using the kymographs shown in A. More than 90 speckles analyzed per condition. (C) Representative kymographs showing random landing along GMPCPP-stabilized microtubule lattices, processive motility, and plus-end accumulation of individual Kip2-WT and Kip2-P1<sup>-</sup> motors. (D) Quantification of Kip2 motor speed using the kymographs shown in C. More than 55 speckles analyzed per condition. Statistical significance was calculated using two-tailed Student's *t* test; \*  $P < 0.05$ ; \*\*  $P < 0.01$ . Source data for C and D are available in Data S1.

Video 1. **A representative time-lapse movie shows Kip3-Kip2-chimera molecules accumulate on microtubule plus-ends.** Corresponds to Fig. S1 D. The movie consists of 80 frames taken every 1.07 s and the frame speed is sped up by threefold for better visualization. Scale bar, 2  $\mu$ m.

Video 2. **Kip2-NMD-mNeonGreen accumulates on both the growing and shrinking cytoplasmic microtubule plus-ends.** The red arrowhead marks the plus-end. SPBs are visualized with Spc72-GFP. Corresponds to Fig. 4 C. The movie consists of 80 frames taken every 1.07 s and the frame speed is sped up by threefold for better visualization. Scale bar, 2  $\mu$ m.

Provided online are Data S1, Table S1, Table S2, Table S3, and Table S4. Data S1 shows quantification of maximum aMT length ( $\mu$ m) in metaphase cells of indicated genotype for Fig. 1 F and Fig. 5 H; quantification of aMT dynamics in wildtype and *kip2* $\Delta$  preanaphase

cells at 30°C for Fig. 1, G–I; normalized GFP fluorescence intensity (%) on aMT plus-ends for Fig. 4 B; ratio of Tubulin intensity over Kip2 or MBP intensity from free GDP-Tubulin co-IP experiment for Fig. 6, C–E and Table S2; quantification of the speeds ( $\mu\text{m}/\text{min}$ ) of GFP speckles moving along aMTs in vivo for Fig. S5, B and D; quantification of the speeds ( $\mu\text{m}/\text{min}$ ) of GFP speckles moving along preanaphase cytoplasmic microtubules for Fig. S2 B; relative Bik1-3xGFP fluorescence (%) associated with bud-directed cytoplasmic microtubules in cells of indicated genotype for Fig. S2 C; and relative Kip2-G374A-3xsfGFP fluorescence (%) associated with bud-directed SPBs in wildtype and *bik1 $\Delta$*  cells for Fig. S2 F. Table S1 shows quantification of preanaphase astral microtubule length and dynamics in living cells. Table S2 shows quantification of microtubule length and dynamics in vitro with 7  $\mu\text{M}$  porcine tubulin. Table S3 lists all recombinant proteins used in in vitro studies. Table S4 shows yeast strains used in this study.